Influence of shell closure on properties of excited nuclear states

V. A. Morozov
Joint Institute for Nuclear Research, Dubna

Fiz. Elem. Chastits At. Yadra **22**, 765–800 (July–August 1991)

The systematics of the experimental data providing evidence of shell and subshell closure in nuclei are reviewed. Different methods of analysis that permit identification of such evidence are listed. The method of differentiating the energy surface of excited states of a definite nature is used for the first time. It has made possible the identification of the closure of shells, subshells, and quasishells in nuclei of the spherical, transitional, and deformed regions. It is found that magnetic transitions of the types $M1$, $M2$, $M4$ can serve as a probe that also permits identification of shell closure in nuclei. It is established that in this case the ratios of the reduced probabilities of proton and neutron transitions for odd $N=Z$ are close to the single-particle limit.

INTRODUCTION

The identification of new magic and half-magic nuclei and the detection of the effects of shell and subshell closure are of great interest for establishing the limits of applicability of the nuclear shell model[1] or its modifications, and also for establishing the number of valence nucleons above the closed nuclear core. In recent years, some experimental and theoretical studies have been devoted to proving the existence of a new magic number $Z = 64$ in $^{146}_{64}Cd_{82}$ (Refs. 2–7). A characteristic feature of this magic number, compared with the magic numbers $Z = 50$ and 82, is the lower stability of the given shell with respect to changes in the numbers of protons and neutrons in the nucleus. Therefore, the identification of new magic numbers relates to the problem of establishing how far the influence of a given closed shell extends in the neighboring nuclei.

The aim of the present work was to select methods for identifying closed shells in nuclei and to analyze some experimental data that indicate closure of nuclear shells and, in particular, closure of the neutron shell with $N = 64$, since according to the shell model closure of the subshells $2d_{5/2}$ and $1g_{7/2}$ (Fig. 1) is to be expected in this case. Figure 1 gives the scheme of excited states of the nuclei after a part that takes into account spin–orbit coupling has been introduced into the potential of the mean field.

1. METHODS OF IDENTIFYING CLOSED SHELLS AND SUBSHELLS IN NUCLEI

The idea of nuclear shell structure arose by analogy with the concept of atomic shell structure as experimental data were accumulated that indicated the existence of definite distinguished numbers of nucleons in nuclei, the so-called magic numbers: 2, 8, 20, 28, 50, 82, and 126. It was noted that if a nucleus contained such a number of nucleons—protons or neutrons—then irregularities would be observed in the behavior of nuclear properties such as the nuclear binding energies, the energies of β and α decay, etc. These phenomena were attributed to closure of nucleon shells in the nuclei. The initial attempts to explain the complete set of magic numbers were not crowned with success. They considered the motion of noninteracting nucleons in the potential of the mean field with allowance for the Pauli principle, varying the form of the nuclear potential from that of a harmonic oscillator to a potential in the form of a rectangular well. It was only after inclusion, in the nuclear potential, of a strong spin–orbit coupling that it became possible to explain the observed values of the magic numbers.

The state of each nucleon in a nucleus with a potential

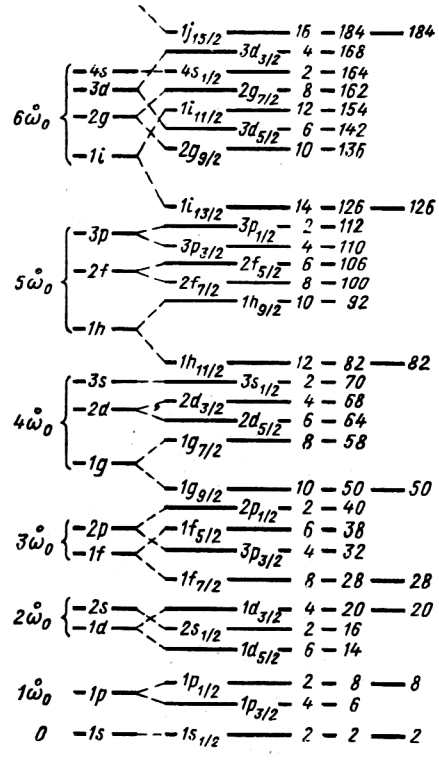

FIG. 1. Scheme of single-particle levels in a potential intermediate between a rectangular and an oscillator well and with spin–orbit coupling.[8]

 0090-4759/91/040367-21$04.00

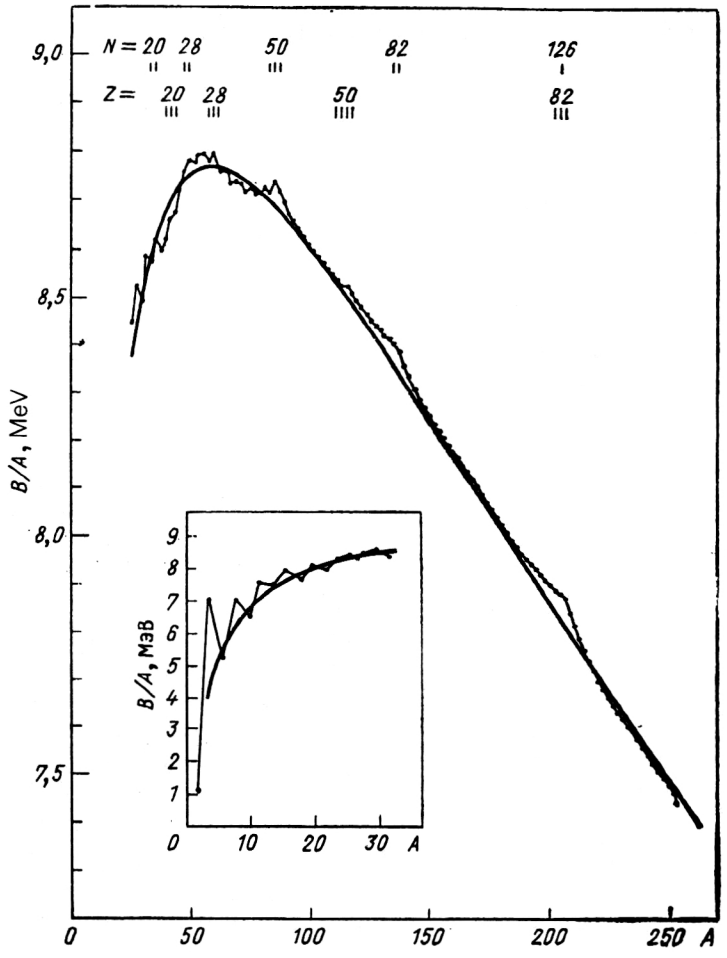

FIG. 2. Binding energies per nucleon, B/A, for the most stable isobars for even values of A.

in the form of an infinite spherically symmetric harmonic-oscillator well can be characterized by the set of quantum numbers (n, l, j, m_j), which determine the sequence of occupation of the orbits and the degree of degeneracy of each state. For different values of the orbital angular momentum l, the following notation is employed:

l=0, 1, 2, 3, 4, 5, 6 ...

s, p, d, f, g, h, i ...

The spin–orbit coupling leads to a lifting of the degeneracy of the states and to grouping of the nucleon energy levels in a comparatively narrow energy interval, and this results in the formation of a magic shell if the energy interval between a given shell and the following shell is sufficiently large. Otherwise, we have closure of a "subshell," which characterizes degenerate states determined by the numbers n and l. We note here a circumstance that was pointed out by Bohr and Mottelson.[9] In nuclei with nonspherical equilibrium shape, the anisotropic part of the potential gives, despite being small compared with the spherical part, shifts of the levels that are comparable with the distance between the shells.

Later in this paper we will demonstrate the energy that characterizes occupation of orbitals by nucleon pairs in deformed nuclei.

We now list the main experimental methods that permit identification of closed shells and subshells in nuclei.

Binding energy of nucleons in the nucleus

Binding energy per nucleon: B/A. The dependence of the binding energy per nucleon for the most stable isobars is shown in Fig. 2 (Ref. 10). The maxima observed in this distribution are associated with the closure of nuclear shells.

Neutron and proton separation energies: S_n and S_p. Figure 3 shows characteristic distributions of the nucleon binding energies, which permit the identification of shell effects.

Separation energies for two nucleons: S_{2n} and S_{2p}. As in the previous case, the corresponding dependence of S_{2n} or S_{2p} on Z or N undergoes a nonmonotonic change in the form of a jump (Fig. 4) on the closure of shells. The systematics of the experimental data on the values of S_n, S_p, S_{2n}, S_{2p} are given in Ref. 11.

Pairing energies. The neutron and proton pairing energies, defined as

$$\Delta_n = -\tfrac{1}{4}\left[S_n(N-1,Z) - 2S_n(N,Z) + S_n(N+1,Z)\right]$$

and

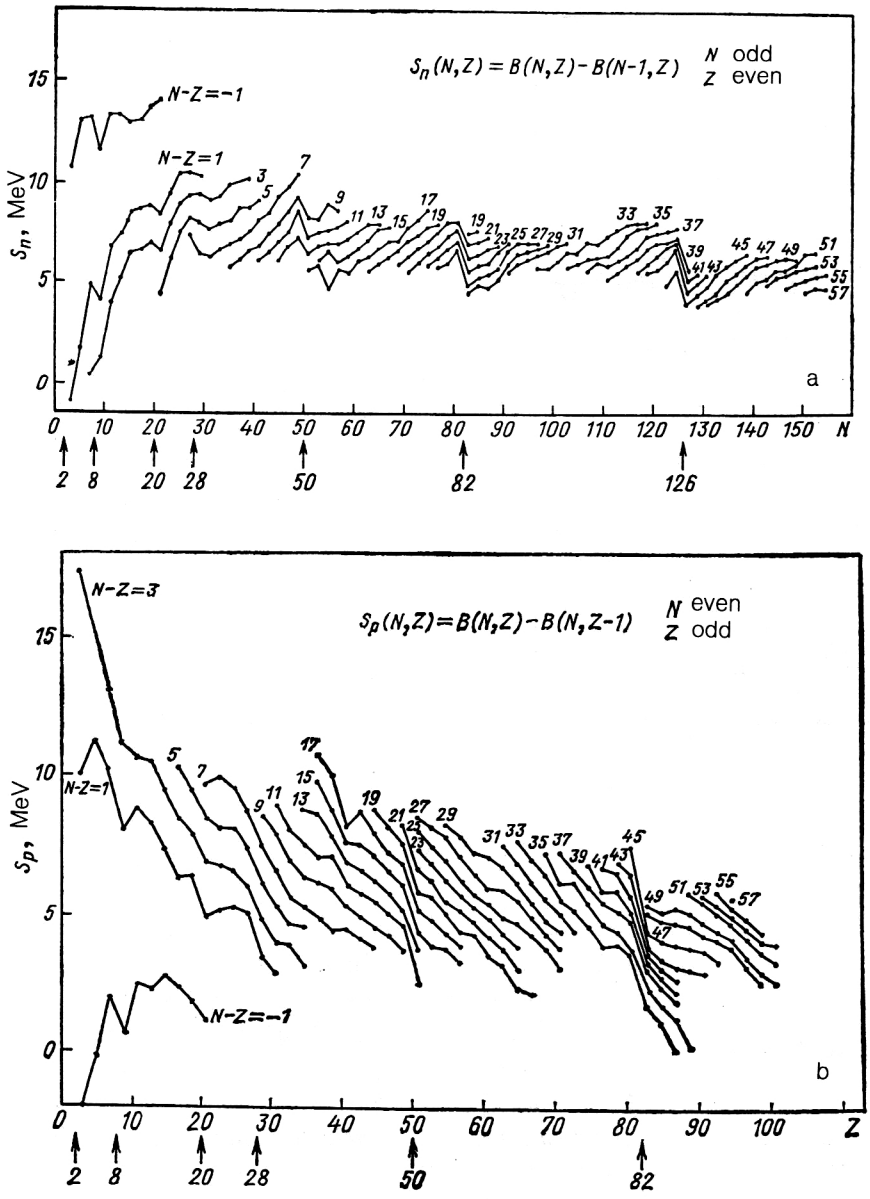

FIG. 3. Separation energies for neutrons, S_n (a), and protons, S_p (b).[10]

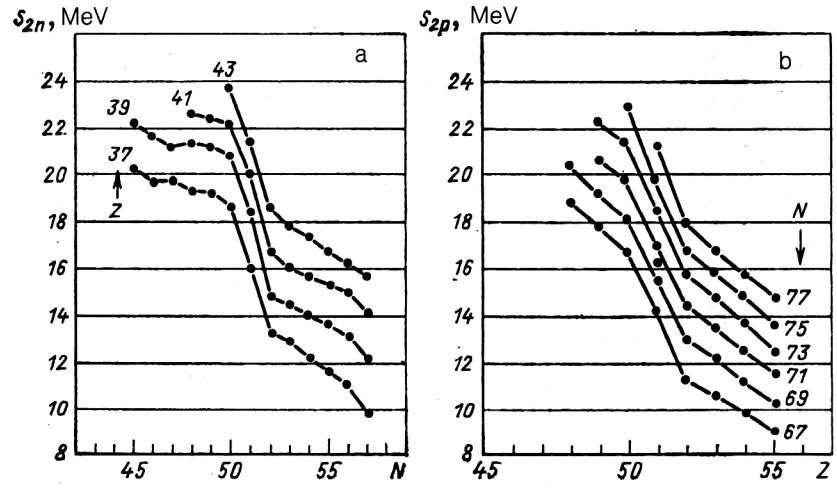

FIG. 4. Separation energies for a pair of neutrons, S_{2n} (a), and a pair of protons, S_{2p} (b) (fragment of figure taken from Ref. 11).

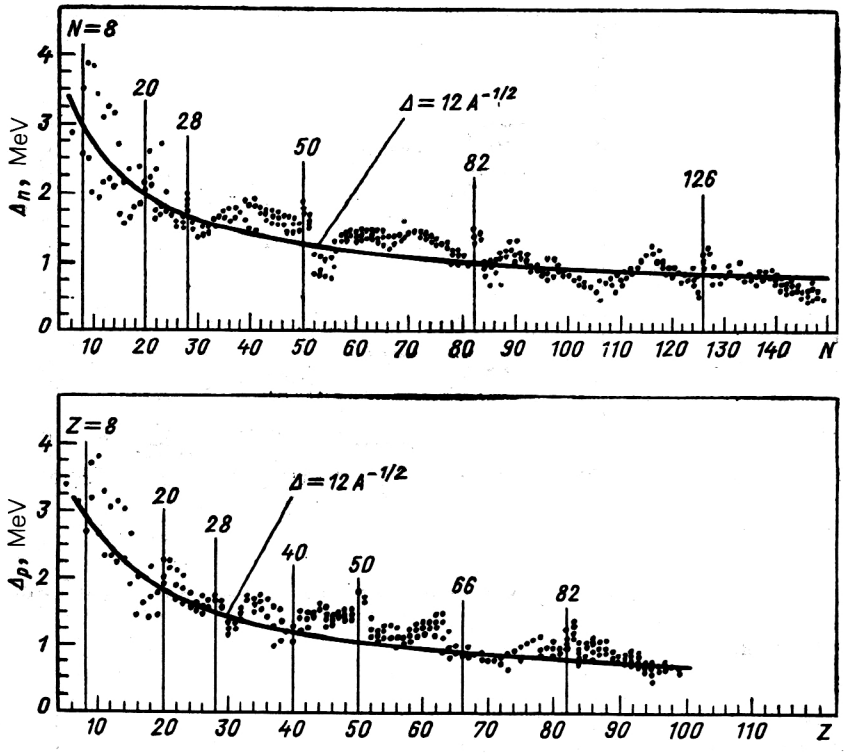

FIG. 5. Dependence of the pairing energies Δ_n and Δ_p on N and Z, respectively.[9]

$$\Delta_p = -\tfrac{1}{4}\,[S_p(N,Z-1) - 2S_p(N,Z) + S_p(N,Z+1)],$$

also exhibit a characteristic dependence on N or Z on the closure of shells in nuclei (Fig. 5).

Decay energy of radioactive nuclides

Energy of β decay. Figure 6 shows the form of dependence exhibited by the β-decay energy on transition through a closed shell.

Energy of α decay. The nonmonotonic nature of the energy dependence of the α decay of nuclides when the number of nucleons is changed is due to shell closure and can be clearly seen in Fig. 7 (Ref. 11).

Systematics of the energies of excited nuclear states

Excited 2^+ and 3^- states in even–even nuclei. The systematics of the energies of these states exhibit the presence of an extremum in the values of the energy as a function of Z or N when a shell is crossed (Fig. 8). To identify closed shells, one can also use the systematics of the ratios $E(4^+)/E(2^+)$ with respect to Z or N.

Excited states in odd nuclei. In odd nuclei, we observe crossing of the particle and hole levels on transition through a closed shell (Fig. 9), owing to the abrupt change in the position of the chemical potential.

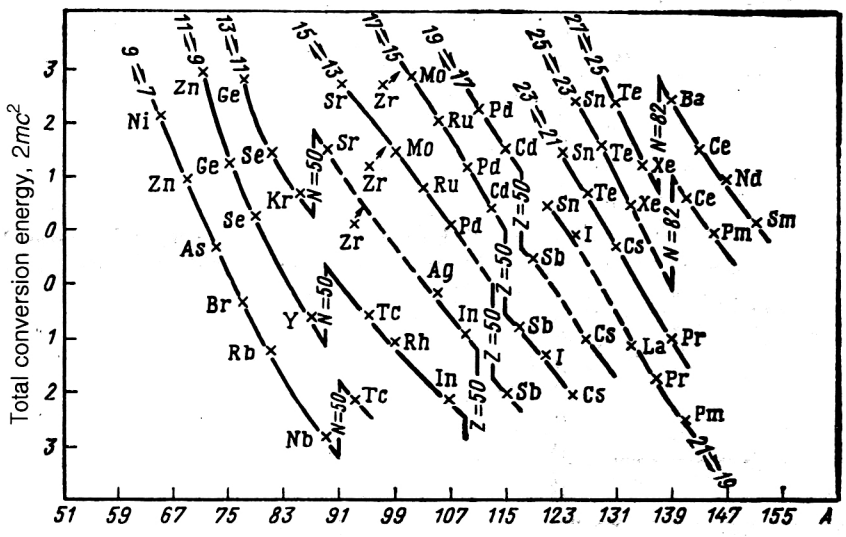

FIG. 6. Energy of a β transition in which an odd neutron is transformed into an odd proton.[12]

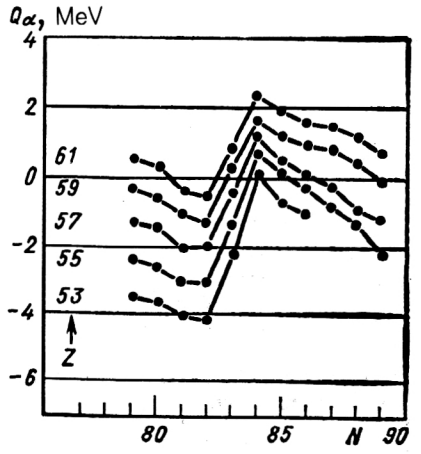

FIG. 7. Energy of α decay as a function of the number of neutrons N (fragment of figure taken from Ref. 11).

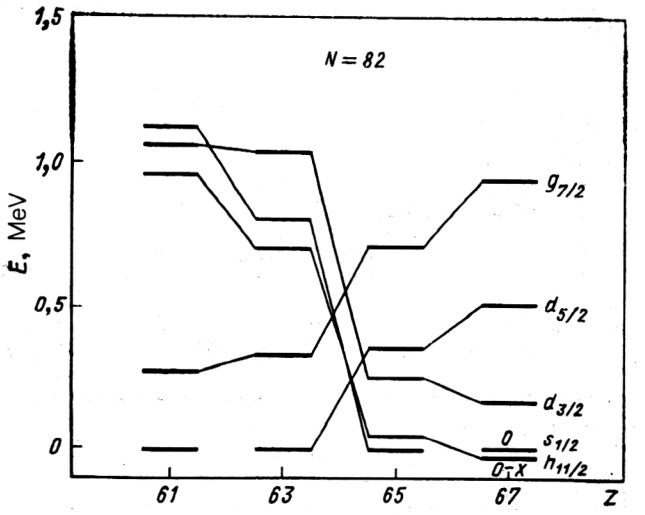

FIG. 9. Energies of single-quasiparticle and hole levels in isotones with $N = 82$.

Reduced widths of α decay and probabilities of electromagnetic transitions

Reduced widths of α decay. These also exhibit a clear structure on the passage through a closed shell (Fig. 10).

Systematics of reduced probabilities of electromagnetic transitions. For multipolarities such as $E0$ in even–even nuclei the systematics of these reduced probabilities also permit identification of closed shells (Fig. 11).

Other methods of determining closed shells

Besides the above methods of identification of closed shells, we can also mention methods based on analysis of the values of the magnetic and quadrupole moments of the nuclear ground states (μ and Q_s),[14] the changes of the mean-square charge radius $\delta\langle r^2\rangle^{A,A+2}$, and analysis of the thickness of the nuclear surface layer[15] and of the density of excited nuclear states in the region of excitation energies of order 5–10 MeV (Ref. 16).

2. INFLUENCE OF SHELL CLOSURE ON THE ENERGIES OF EXCITED STATES IN NUCLEI

Odd nuclei

When the number of protons or neutrons is varied systematically, passage through a closed shell (or subshell) of the nucleus is characterized for odd nuclei by the crossing of some levels. As we have already noted, this is explained by the abrupt change of the chemical potential in the nucleus on such a transition. Tracing the changes in the positions of the levels from nucleus to nucleus, one can identify shell closure. Shell closure is most clearly exhibited in a difference energy analysis,[40] which characterizes the change in the positions of levels of a definite nature in isotopes or isotones. The difference is defined as

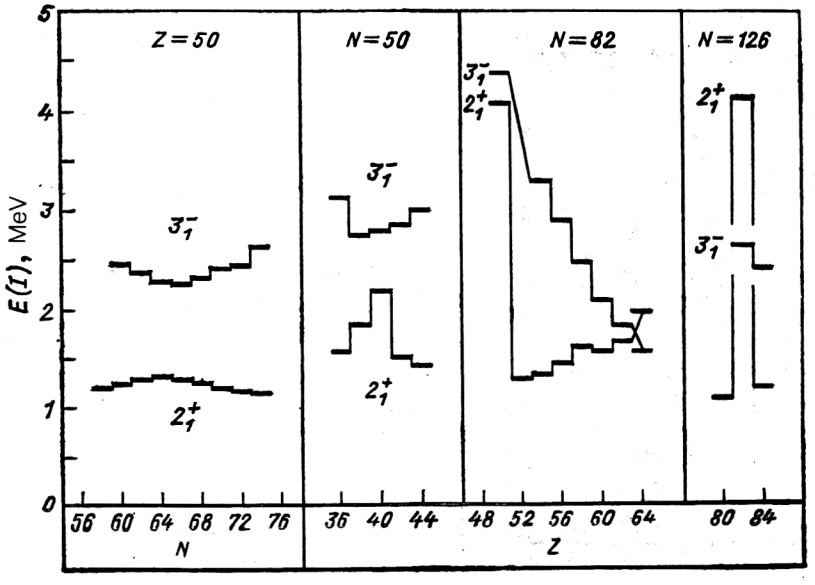

FIG. 8. Schematics of excited states with I^π equal to 2^+ and 3^- in magic and nearly magic nuclei.

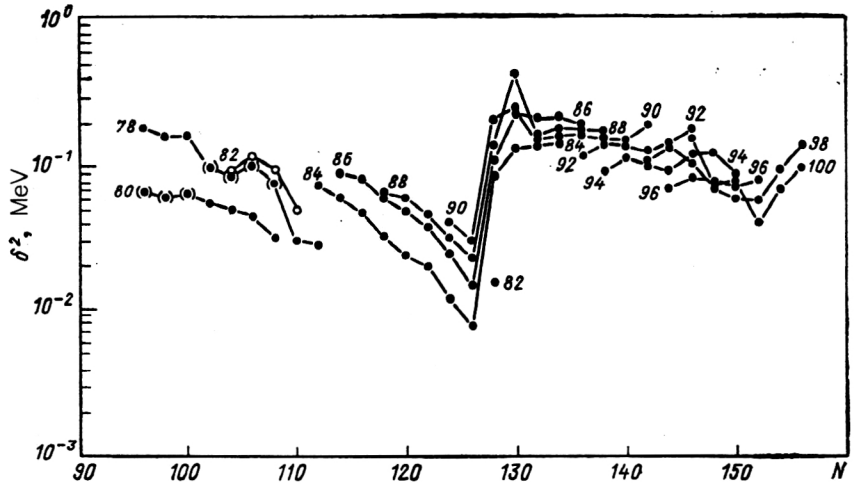

FIG. 10. Reduced α-decay widths (fragment of figure taken from Ref. 13). Estimated data are given in the brackets.

$$\Delta E(I)^{A,A+2}=E(I)^{A}-E(I)^{A+2},$$

where I is the spin of a definite state in the nucleus, and E is the energy of this state. Effectively, the $\Delta E(I)^{A,A+2}$ diagram represents differentiation of the energy surface (DES) of levels of a definite spin, realized through proton sections of isotones or through neutron sections of isotopes. Analysis of the DES diagrams permits identification of shell or subshell closure in both odd and even–even nuclei. What levels can be used to construct DES diagrams? In odd spherical nuclei, shell closure can be established from the DES diagrams of the single-particle levels. In even–even spherical nuclei, one can use in the analysis single- and two-photon levels of quadrupole vibrations, and also octupole states. In the analysis, one can also use the quasirotational levels of the corresponding states in order to establish not only the fact of shell closure but also the structural changes that occur in the corresponding band.

A similar approach can also be used to establish quasishells in deformed nuclei. Figure 12a is an example of the rearrangement of the system of levels in odd nuclei with a closed neutron shell ($N=126$) on the passage through a different, proton closed shell with $Z=82$. The grouping of the particle and hole levels at the zero line at $Z=83$ indicates stabilization of the positions of both these and other levels in nuclei with Z equal to 83 and 85 on the passage through the closed shell with $Z=82$.

We also observe such behavior on passing through the shell with $Z=64$ (Fig. 12b) in odd nuclei with $N=82$. On closure of the neutron shell in odd nuclei with $Z=50$, the DES diagram has a different form (Fig. 13a), namely, the particle levels reveal closure of the neutron shell at $N=62$, the hole levels at $N=64$, while $N=66$ corresponds to closure of the neutron shell on the basis of both the particle and the hole levels. This difference is obviously due to the different sequence of subshell closure in isotones with $N=82$ ($Z=59$–67) and isotopes with $Z=50$ ($N=59$–71). The $s_{1/2}$ orbital in isotopes with $Z=50$ is closed beginning with ^{113}Sn ($N=63$), but in the isotones with $N=82$ the $s_{1/2}$ orbital is observed only from $Z=65$ in ^{147}Tb. However, a common feature in all these cases of analysis of the DES diagrams is the separate grouping of the $\Delta E(I)^{A,A+2}$ values for the particle and hole levels in a comparatively narrow energy interval before the shell closure and the fused grouping of both types of level around the zero value after the shell closure. The stability of the neutron shells at $N=62$–64–66 can be estimated by changing Z successively from the magic number by 2. For example, we can take Z equal to 48 and 52, etc. Figure 13b shows one of the cases. It can be seen that already at $Z=48$ the stabilizing influence of the proton shell on the closure of the neutron shell disappears.

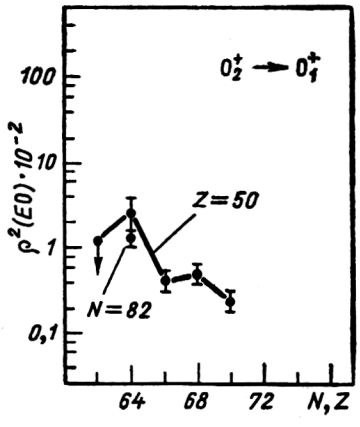

FIG. 11. Electric monopole transitions in Sn and Gd isotopes.

Even–even nuclei

Nuclides from the spherical and transitional region of nuclei. The rearrangement of the shells is seen particularly clearly in analysis of the DES diagrams in even–even nuclei. Figure 14 shows the diagrams for the lowest levels with I^{π} equal to 2_1^+, 4_1^+, 3_1^- in isotopes of nuclei with Z equal to 80, 82, 84. The energies of the corresponding states are taken from Ref. 17. A characteristic feature is the

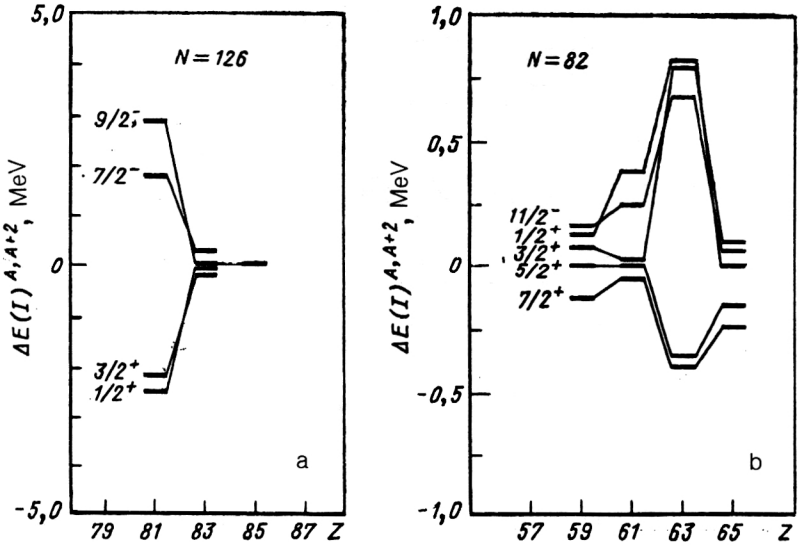

FIG. 12. DES (differentiation of the energy surface) diagram for odd isotones of nuclei with $N = 126$ (a) and $N = 82$ (b).

change of $\Delta E(I)^{A,A+2}$ in phase for states with I, π equal to 2_1^+, 4_1^+ from a negative to a positive value on passage through the closed shell. This difference reaches its maximal value at $N = 126$, and, moreover, for the doubly magic nuclei the negative and positive values of $\Delta E(I)^{A,A+2}$ are approximately equal in absolute magnitude. For the $I^\pi = 3_1^-$ states, the behavior of $\Delta E(I)^{A,A+2}$ is similar, although in this case crossing of the zero level does not occur. A change from $Z = 82$ by ± 2 units leads to a significant decrease of the shell closure effect. The DES diagrams in the region of lighter nuclei exhibit similar behavior on the closure of shells with N equal to 20, 28,, 50, 56 (Figs. 15 and 16). Note that for nuclei with $Z = 20$ on closure of the shells with $N = 20$ and 28 there is a variation of $\Delta E^{A,A+2}$ in phase for the states with I^π equal to 0_2^+, 2_2^+, 3_1^-. Change of the Z of the nucleus by ± 2 units from $Z = 20$ leads to a significant reduction in the effect of shell closure, as for the case $Z = 82 \pm 2$. Examination of the isotopes with $Z = 40$ reveals a similar picture, except that the $I^\pi = 3_1^-$ states do not exhibit closure of a subshell with $N = 56$, in contrast to the states with I^π equal to 2_1^+, 4_1^+, 0_2^+, the behavior of which clearly demonstrates closure of a subshell with $N = 56$. One may also note an observable effect of closure of a proton subshell at $Z = 38$. In Table I we list the states in various quasirotational and vibrational bands from which one can identify closed shells in even–even nuclei with $A = 76$–100, and also in lighter nuclei with $A = 12$–50, which will be considered later.

Examination of the DES diagrams for the isotones with N equal to 82, 82 ± 2 in the region of $Z = 64$ (Fig. 17) makes it possible to establish closure of subshells at $Z = 58$ from the states with $I^\pi = 2_1^+$ and at $Z = 64$ from the states with I^π equal to 2_1^+, 4_1^+, and 3_1^-. A distinctive feature in this case is the variation in antiphase of the difference of the energy of the states with $I^\pi = 3_1^-$ with respect to the states with I^π equal to 2_1^+ and 4_1^+, in contrast to the cases

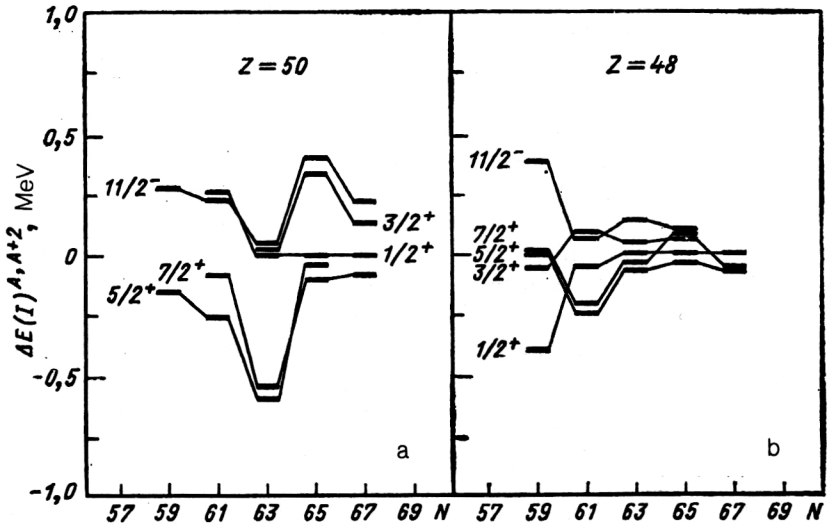

FIG. 13. DES diagrams for odd isotopes of nuclei with $Z = 50$ and $Z = 48$.

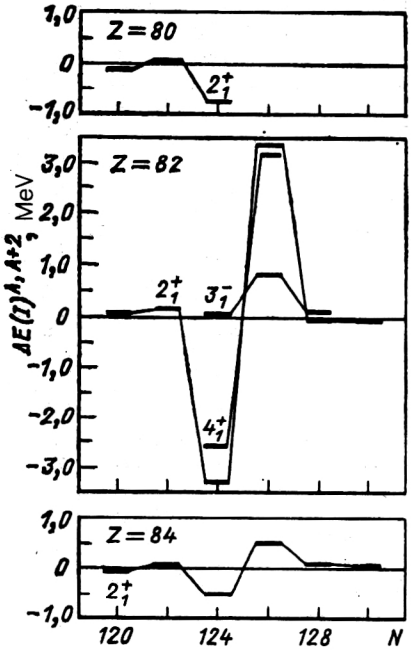

FIG. 14. DES diagrams for even–even isotopes of nuclei with $Z = 80$–84.

considered earlier. One may also note the significantly smaller effect of the shell closure at $Z = 64$, which is completely smeared for a change of the neutron number from $N = 82$ by ± 2 units. In fact, this indicates that it is not a shell but a subshell that is closed at $Z = 64$. The same conclusion was reached in Ref. 18. Closure of a proton subshell at $Z = 58$ is also confirmed by the diagram presented in Fig. 18.

On the basis of the considered cases, we can turn to analysis of the closure of the neutron shell in the tin isotopes at $Z = 50$ (Fig. 19). We establish that in the tin isotopes closure of only subshells is observed, and the effect of the closure is smaller not only compared with the doubly magic nuclei but also with ^{146}Gd. The behavior of the states with $I^\pi = 4_1^+$ confirms, as in the odd tin isotopes, closure of a subshell with $N = 62$. The states with $I^\pi = 2_1^+$ reveal closure of a subshell with $N = 64$, and the states with I^π equal to 4_1^+ and 3_1^- confirm, as in the odd tin isotopes, closure of a subshell with $N = 66$. Inclusion in the analysis of the shell closure of states with I^π equal to 6_1^+ and 2_2^+ makes it possible to establish, besides the shells already identified, closure of neutron quasishells in the Sn isotopes for N equal to 60, 68, and 72 (Table II). The systematic identification of neutron shells in the Sn isotopes on closure of the neutron orbitals by nucleon pairs is a significant difference from previously considered examples.

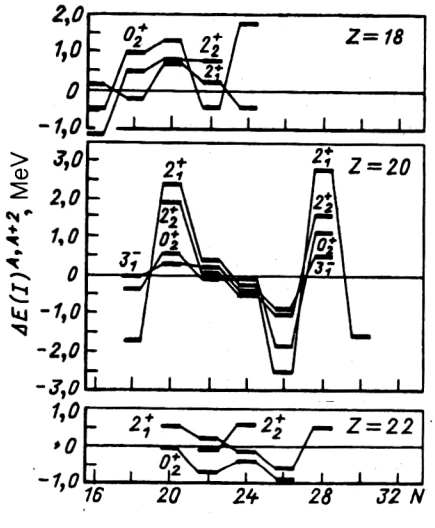

FIG. 15. DES diagrams for even–even isotopes of nuclei with $Z = 18$–22.

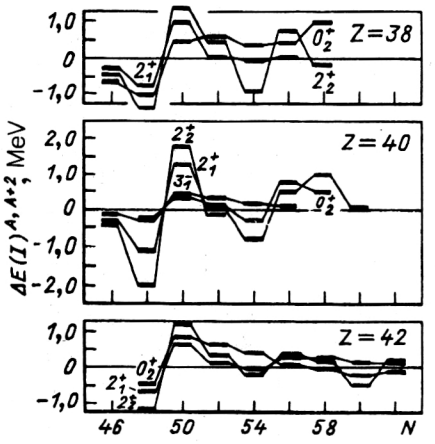

FIG. 16. Diagrams for even–even isotopes of nuclei with $Z = 38$–42.

If we examine the DES diagram for the chain of isotopes at $Z = 50 \pm 2$, we see abrupt structural changes of the diagrams. At $Z = 48$ there remains only the subshell with $N = 62$, and at $Z = 52$ there may only remain the subshell with $N = 66$.

Light even–even nuclei with $N=Z$. Analysis of the DES diagrams in light even–even nuclei with $N=Z$ made it possible to establish closure of shells at $N=Z$ from the levels of the quasi-β-vibrational and quasi-γ-vibrational states (Table I, Fig. 20).

Deformed nuclei. Analysis of the DES diagrams also makes it possible to identify quasishells in even–even deformed nuclei. In this case, the analysis can be made using excited states of rotational bands of the ground or β- or γ-vibrational states. Note the way in which the number $N = 86$ is distinguished in the transitional region of nuclei for Z equal to 64, 66, 68. As an example, Fig. 21 gives the DES diagram for Dy isotopes. In the diagram we can clearly trace the connection between states with definite spin and closure of a neutron shell. Analyzing the DES diagrams (Fig. 22), we can establish closure of quasishells in the deformed nuclei for N equal to 94, 98, 100, 102, 104, 106, 108, 110, 112, 114, 116, 118, 120, 122 (Table III). For

TABLE I. Excited states of nuclei from which neutron shells and subshells in even–even nuclei with $Z = 6$–22 and $Z = 36$–44 have been identified.

Neutron shells	Z = 6	8	10	12	14	16	18	20	22
6	0_2^+ 2_1^+								
8		0_2^+, 2_2^+							
10			0_2^+						
12				0_2^+ 2_1^+					
14					0_2^+ 2_1^+				
16						2_1^+, 2_2^+ 0_2^+			
18				2_1^+			0_2^+, 2_2^+ 2_1^+ 0_2^+		
20								0_2^+, 2_1^+, 3_1^-	
24								2_1^+, 0_2^+, 2_2^+, 3_1^-	2_2^+ 2_1^+
28									
	36	38		40		42		44	
40	2_1^+								
50	2_1^+, 2_2^+	2_1^+, 0_2^+, 2_2^+ 2_1^+, 2_2^+		2_1^+, 0_2^+, 2_2^+ 2_1^+, 0_2^+		2_1^+, 0_2^+, 2_2^+ 2_1^+, 2_2^+		2_1^+, 0_2^+, 2_2^+	
56									

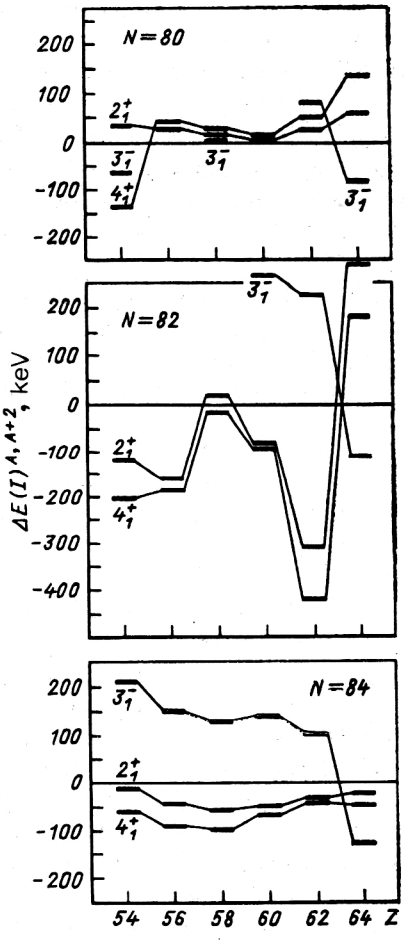

FIG. 17. DES diagrams for even–even isotopes of nuclei with $Z = 80$–84.

comparison, Table III also gives data on nuclides with $N = 86$ and $Z = 82$. The connection between quasishells and vibrational states of different types is interesting. In several nuclei, the numbers N equal to 98, 106, 116, 118 are distinguished only through the β-vibrational states, while the γ-vibrational states in the same nuclei do not enable us to establish closure of quasishells. Note that a shell with $N = 106$ is also manifested in ^{186}Hg, as is indicated by the abrupt fall in the mean-square charge radius on the tran-

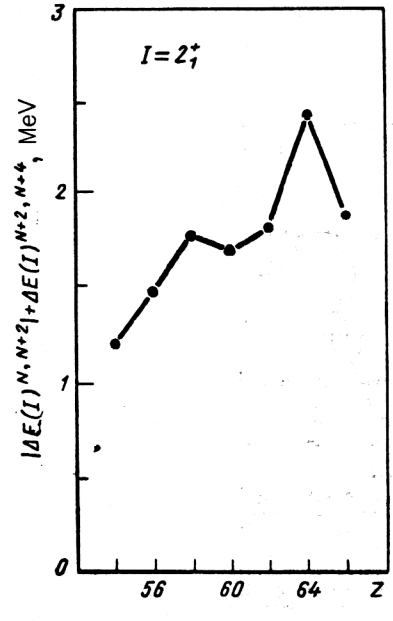

FIG. 18. DES diagram for states with $I^\pi = 2_1^+$ in nuclei with $Z = 54$–66 ($N = 80$).

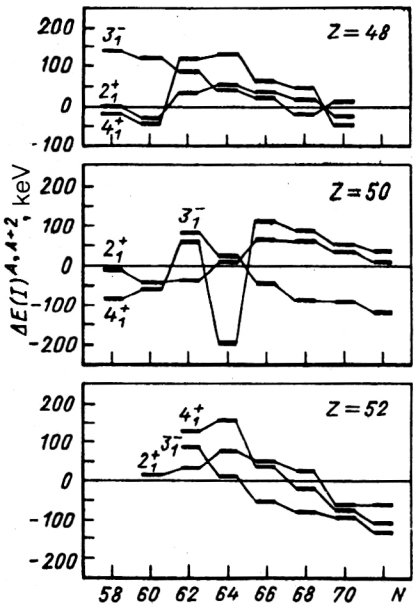

FIG. 19. DES diagrams for even–even isotopes of nuclei with $Z = 48$–52.

sition from ^{185}Hg to ^{186}Hg (Ref. 19). In the quoted study, the drop is interpreted as a transition from a strongly deformed prolate shape of the nucleus to a weakly deformed oblate shape. The numbers $N = 104$, 108, 114, 120 are identified only by the γ-vibrational states and not by the β-vibrational states. An exception is the number $N = 94$, which is identified by the γ- and β-vibrational states in ^{160}Dy, and $N = 112$, which is identified by a β-vibrational state in ^{188}Os and a γ-vibrational state in ^{192}Hg. The remaining quasishells can be identified by the excited levels of the rotational bands of the ground states.

It is an interesting fact that from $N = 98$ and to $N = 122$ the addition of each new pair of neutrons is manifested as closure of a shell in a spherical nucleus. Thus, lifting of the level degeneracy as a consequence of deformation of the nuclei can be deduced from the DES diagrams for different states of rotational bands in deformed nuclei. It is important to note that the effect of quasishell

TABLE II. Excited states of nuclei from which neutron shells and subshells in even–even nuclei with $Z = 48$–52 were identified.

	Neutron shells					
Z	60	62	64	66	68	72
48		2_1^+ 4_1^+			3_1^-	
50	6_1^+	4_1^+	2_1^+, 2_2^+	4_1^+, 3_1^-	2_1^+	2_2^+
52				3_1^-		

closure in deformed nuclei is appreciably less in the $\Delta E(I)^{A,A+2}$ magnitude than the effect of shell closure in doubly magic nuclei, but it is comparable with the effect of shell closure in half-magic nuclei. It is obvious that closure of different orbitals of the considered nuclei is manifested only for definite states and for a definite nature of the nucleon–nucleon interaction in the nucleus or for a definite nature of the motion of the nuclear matter. We emphasize the need for further accumulation of experimental data in order to establish the range of influence of quasishells in Z on the levels of rotational bands of different natures.

3. PROBABILITIES OF ELECTROMAGNETIC TRANSITIONS IN SOME MAGIC AND NEARLY MAGIC NUCLEI

Reduced probabilities of *E*0, *E*2, and *E*3 transitions

Comparison of the reduced probabilities of electromagnetic transitions of the same type in magic and half-magic nuclei and in the region of mass numbers near $Z = 50$, $N = 64$, $Z = 64$, $N = 82$, and $Z = 82$, $N = 126$ establishes that they are qualitatively consistent. In Table IV (Refs. 12–16) and in Figs. 23 and 24, we give data that characterize electric quadrupole and octupole transitions to 2_1^+ and 3_1^- states of even–even nuclides. At the present time, there are no data on the lifetime of the 2_1^+ state in ^{146}Gd, but it can be seen that the isotones with $N = 82$ and Z

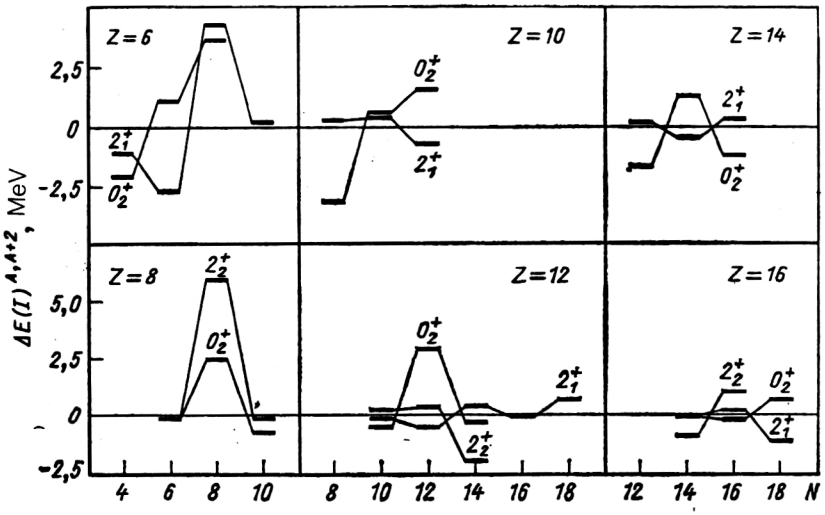

FIG. 20. DES diagrams for even–even isotopes of nuclei with $Z = 6$–16.

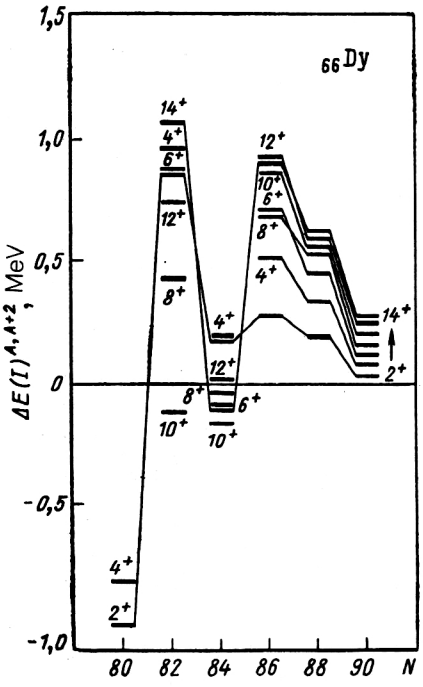

FIG. 21. DES diagram for even–even isotopes of Dy.

equal to 60 and 62 have the same order of enhancement of the $E2$ transition as the Sn isotopes with N equal to 60 and 62. We note that in the doubly magic nucleus ^{208}Pb the 2_1^+ state is less collectivized [$S(E2)_W = 8.7$ (in Weisskopf units)] than for the other considered nuclides [$S(\sigma L)_W = B(\sigma L)_{exp}/B(\sigma L)_W$]. The 3_1^- states in ^{114}Sn, ^{146}Gd, and ^{208}Pb are also collectivized, moreover to a greater degree in ^{114}Sn than in ^{146}Gd and ^{208}Pb. For the electric monopole transitions $E0(0_2^+ - 0_1^+)$ (Fig. 11) we also observe a growth in the value of the square ρ^2 of the reduced nuclear matrix element of the $E0$ transition at $N = 64$. To within the errors, this value for ^{114}Sn is equal to the value of ρ^2 for ^{146}Cd.

Reduced probabilities of *M*2 transitions

Table V (Refs. 21–26) and Figs. 25 and 26 give the reduced probabilities of neutron and proton transitions of the type $M2(1h_{11/2}-1g_{7/2})$ for nearly magic nuclei near Z, $N=64$ as functions of N and Z. The characteristic features of the dependence are shown in general form in Fig. 27, which shows schematically that the reduced probability of the $M2$ transitions is minimal precisely at the saddle point at which two closed shells cross.[41] This behavior of the $B(M2)$ transition probability in odd nearly magic nuclides

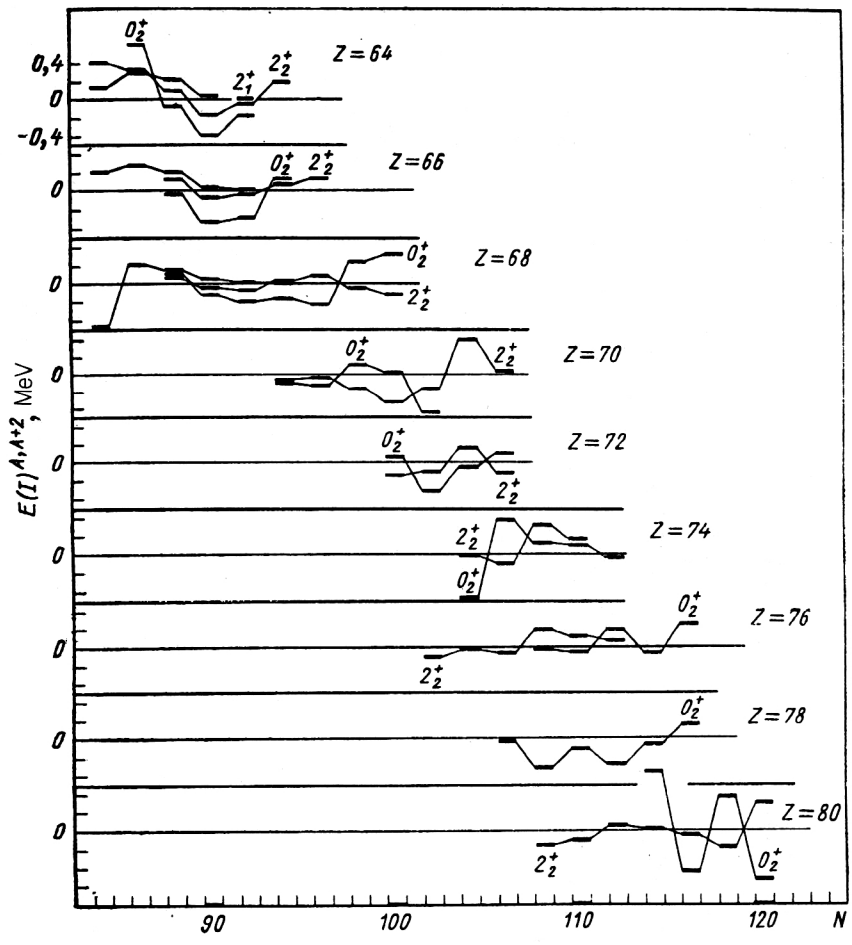

FIG. 22. DES diagrams for even-even deformed nuclei (the energy scale for all cross sections is the same).

TABLE III. Excited states of nuclei from which neutron quasishells in even–even nuclei with $Z = 64$–82 were determined.

Neutron shells	Z = 64	Z = 66	Z = 68	Z = 70	Z = 72
86	6_1^+	6_1^+, 8_1^+, 10_1^+, 14_1^+	2_1^+, 4_1^+, 8_1^+,		
94	γ_1 (2⁺, 3⁺)	γ_1 (2⁺, 3⁺), β_1 (0⁺, 2⁺)	10_1^+, 16_1^+		
98			γ_1 (2⁺, 3⁺)	β_1 (0⁺)	
100			β_1 (0⁺—4⁺)	g (10⁺—14⁺)	g (10⁺—20⁺)
102			g (6⁺—10⁺)	g (16⁺)	
104				γ_1 (2⁺—4⁺)	γ_1 (2⁺—4⁺)
106				g (6⁺)	β_1 (0⁺—4⁺)
	Z = 74	Z = 76	Z = 78	Z = 80	Z = 82
100		g (20⁺, 22⁺)			
102		g (16⁺, 18⁺)			
104	g (8⁺—18⁺)	g (4⁺, 6⁺, 14⁺)			
106	β_1 (0⁺, 2⁺)	g (8⁺)			
108	γ_1 (2⁺—6⁺)	γ_1 (2⁺—6⁺)	γ_1 (3⁺)	g (6⁺)	
110			g (12⁺)	g (8⁺)	
112		β_1 (0⁺, 2⁺)	g (10⁺)	g (6⁺) γ_1 (2⁺)	
114		γ_1 (6⁺)		g (2⁺, 4⁺, 18⁺)	4_1^+
116		β_1 (0⁺)	β_1 (0⁺, 2⁺)		2_1^+
118				g (6⁺) β_1 (0⁺)	
120				γ_1 (2⁺, 3⁺)	
122				g (2⁺)	
126					2_1^+

makes it possible to estimate the influence of the magic core on the relative rates of the proton and neutron transitions.

When calculated in the framework of the single-particle model, the ratios of the reduced probabilities of magnetic transitions in a nucleus found in accordance with Moszkowski's scheme are

$$\frac{B(ML)_p^{\mathrm{M}}}{B(ML)_n^{\mathrm{M}}}=\frac{M_\mu^p}{M_\mu^n}\left(\frac{A_p}{A_n}\right)^{\frac{2L-2}{3}}\frac{S_p(I_iLI_j)}{S_n(I_iLI_j)}. \qquad (1)$$

For the transitions that we considered $L=|I_i-I_f|$, and therefore $M_\mu=[L\mu-(g_lL/(L+1))]^2$, $R=r_0A^{1/3}$,

TABLE IV. Electric multipole transitions $E0$, $E2$, $E3$ in magic and nearly magic nuclei.

Z	A	$E0$ $(0_2^+-0_1^+)$		$E2$ $(2_1^+-0_1^+)$		$E3$ $(3_1^--0_1^+)$	
		$E(0_2^+)$, keV	$\rho^2\cdot10^{-2}$	$E(2_1^+)$, keV	S_W	$E(3_1^-)$, keV	S_W
$_{50}$Sn	112	2191	1,2	1257	1,4 (4) (+1)	2355	—
	114	1923	2,6 (13)	1300	1,5 (3) (+1)	2275	9 (4) (+1)
	116	1757	0,44 (9)	1294	1,25 (3) (+1)	2266	3,9 (16) (+1)
	118	1758	0,52 (13)	1230	1,18 (5) (+1)	2328	2,2 (4) (+1)
	120	1875	0,26 (7)	1172	1,1 (2) (+1)	2400	1,8 (2) (+1)
	122	2088	—	1140	1,06 (3) (+1)	2492	2,2 (3) (+1)
	124	(2129)	—	1132	9,0 (2) (0)	2162	3,1 (8) (+1)
$_{60}$Na	142	2217	—	1576	1,20 (2) (+1)	2084	2,86 (+1)
$_{62}$Sm	144	2478	—	1660	1,16 (3) (+1)	1810	—
$_{64}$Gd	146	2165	1,22 (13)	1971	4 (−1)	1579	3,6 (4) (+1)
$_{82}$Pb	206	—	—	4085	8,7 (5) (0)	2614	3,39 (5) (+1)

Note. The notation $S_W = 9(4)(+1)$ is equivalent to $S_W = (9\pm4)\times10^1$.

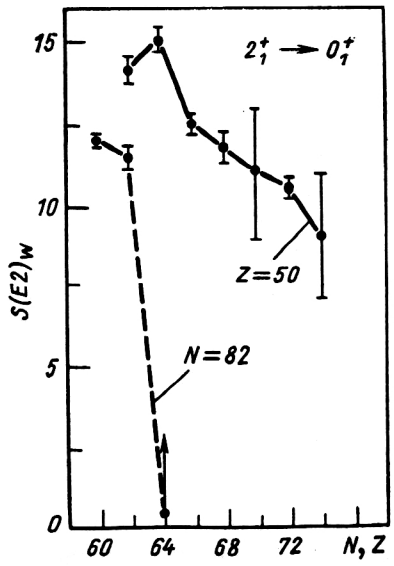

FIG. 23. Enhancement factors of electric quadrupole transitions for isotopoes with $Z = 50$ and isotones with $Z = 82$.

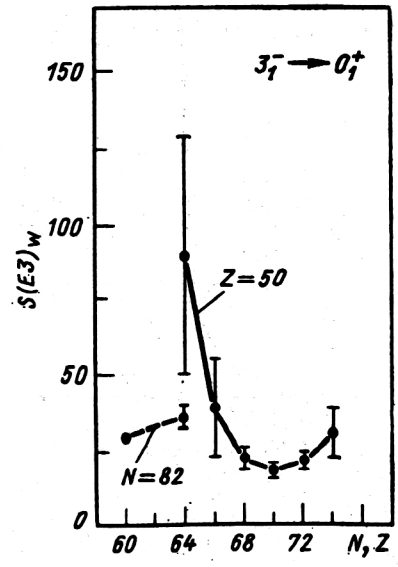

FIG. 24. Enhancement factors for electric octupole transitions for isotopes with $Z = 50$ and isotones with $N = 82$.

where $r_0 = 1.2$ fm, and $S(I_i, LI_f)$ is the statistical factor. Allowance for the statistical factor in the analysis of transitions with $I_i^p \neq I_i^n$ and $I_f^p \neq I_f^n$ is justified only in the case of a radiative transition of one particle, but since in the majority of cases nuclear states have a more complicated nature, allowance for the factor $S(I_i, LI_f)$ is often unjustified. Therefore, as is often done, we take the ratio $S_p/S_n = 1$. In this case

TABLE V. Reduced probabilities of neutron and proton $M2$ transitions of the type $1h_{11/2} \leftrightarrows 1g_{7/2}$ in odd nuclei.

Z	A	E_i/E_f (keV)	$2I_i^\pi$	S_W
$_{48}$Gd	107	845/215	11^-	1,74 (12) (−1)
	109	462/203	11^-	9,3 (8) (−2)
$_{50}$Sn	109	1256/0	11^-	1,4 (2) (−1)
	111	979/0	11^-	1,6 (2) (−1)
	113	738/77	11^-	1,25 (3) (−1)
	115	713/613	11^-	1,20 (1) (−1)
	117	712/315	7^-	1,8 (5) (−1)
	119	787/90	7^-	2,0 (7) (−1)
	121	926/6	7^-	3,2 (8) (−1)
$_{52}$Te	115	280/0	11^-	8,5 (3) (−2)
$_{59}$Pr	135	358/246	11^-	6,1 (6) (−2)
	137	563/231	11^-	8 (3) (−1)
	139	822/114	11^-	1,31 (3) (−1)
	141	1116/145	11^-	2,42 (18) (−1)
$_{61}$Pm	141	629/197	11^-	1,40 (7) (−1)
	143	960/272	11^-	2,5 (2) (−1)
	145	794/61	11^-	2,6 (3) (−1)
	147	649/0	11^-	1,4 (2) (−1)
	149	240/0	11^-	2,3 (2) (−2)
$_{63}$Eu	143	389/272	11^-	8,5 (1) (−2)
	145	716/329	11^-	1,87 (11) (−1)
	147	625/229	11^-	1,10 (2) (−1)
	149	496/150	11^-	6,8 (1) (−2)

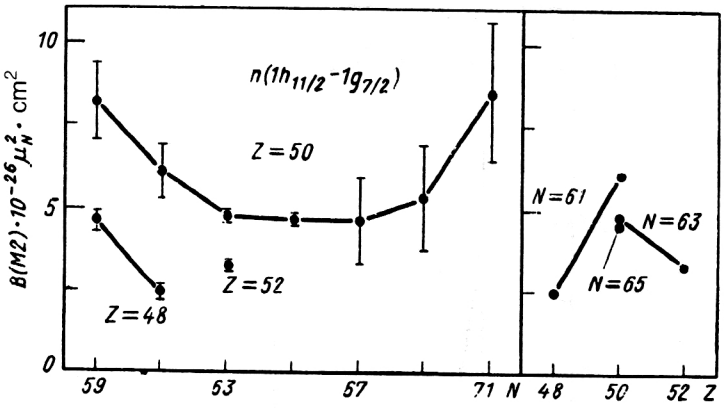

FIG. 25. Reduced probabilities of neutron transitions of the type $M2$ $(1h_{11/2}-1g_{7/2})$.

$$\frac{B(ML)_p^{\mathrm{M}}}{B(ML)_n^{\mathrm{M}}}=\frac{M_\mu^p}{M_\mu^n}\left(\frac{A_p}{A_n}\right)^{\frac{2L-2}{3}}. \tag{2}$$

For the limiting case when we consider transitions of single nucleons or transitions in mirror nuclei

$$B(ML)_p^{\mathrm{M}}/B(ML)_n^{\mathrm{M}}=M_\mu^p/M_\mu^n. \tag{3}$$

These ratios, characterizing transitions of single nucleons for $L=|I_i-I_f|$, are given in Table VI (Ref. 27). It can be assumed that if the given experimental value of this ratio, which is obtained by eliminating the dependence of $B(ML)_{\mathrm{exp}}$ on the mass number A, agrees with the single-particle estimate, then the corresponding transitions can be regarded as transitions of single nucleons. Note that when we calculate $[B(ML)_p/B(ML)_p]_{\mathrm{id}}^{\mathrm{exp}}$ we obtain

$$\left[\frac{B(ML)_p}{B(ML)_n}\right]_{\mathrm{id}}^{\mathrm{exp}}=\left[\frac{B(ML)_p}{B(ML)_n}\right]_{\mathrm{exp}}\left(\frac{A_n}{A_p}\right)^{\frac{2L-2}{3}}=\frac{S_{\mathrm{W}}^p}{S_{\mathrm{W}}^n}. \tag{4}$$

The single-particle estimates given in Table VI were not in fact used to compare the reduced probabilities of proton and neutron transitions, since there was no criterion that permitted a correct comparison of proton and neutron transitions of the same type in nuclei with odd $N=Z$. We can now formulate this criterion to establish a correspondence with calculations in accordance with the single-particle model: The reduced probabilities of neutron and proton transitions of the same type must be compared at the saddle points and in the immediate vicinity of them (Fig. 27), where they take extremal values. At the same time, in a nucleus with an odd number of neutrons the proton shell must be closed, and the other, neutron shell must differ from a completely closed shell by ± 1, ± 3 nucleons, etc. Similarly, in an odd-proton nucleus the neutron shell must be closed, and the proton shell must differ from a completely closed shell by ± 1, ± 3 nucleons, etc.

As an example, Fig. 28 gives the relative probabilities of proton and neutron $M2$ transitions in nuclei for which one, three, or five nucleons are required to close $N_1=Z=64$ shells. The analysis shows that shell closure has a significant influence on the rates of $M2$ transitions. It is found that in odd nuclides with a doubly magic core the experimental value of the ratio of the reduced probabilities of proton and neutron $M2$ transitions is equal to the single-particle limit of these ratios.

Confirmation of this is also provided by analysis of the

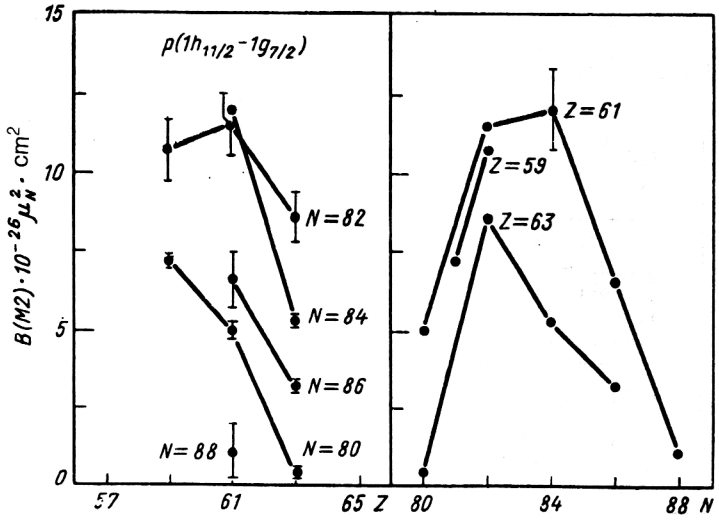

FIG. 26. Reduced probabilities of proton transitions of the type $M2$ $(1h_{11/2}-1g_{7/2})$.

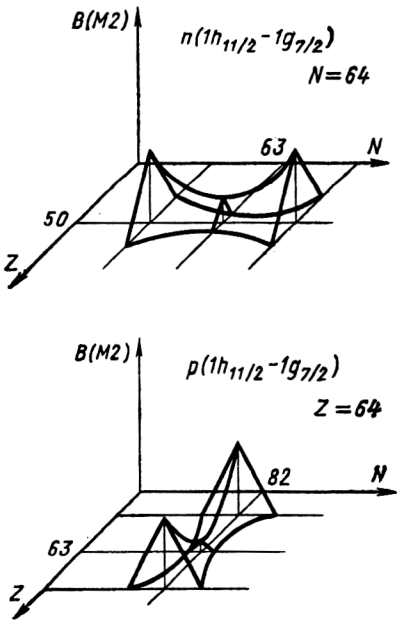

FIG. 27. General form of the dependence of the reduced probabilities of transitions of the type $M2$ ($1h_{11/2}$–$1g_{7/2}$) in odd nuclei with a half-magic core near $N=Z=64$.

probabilities of $M2$ transitions of the type $1f_{7/2}$–$1d_{3/2}$ in mirror nuclei for which one particle is lacking to make the doubly magic cores $^{39}_{19}K_{20}$ and $^{39}_{20}Ca_{19}$ (Table VII).[28–31] The value obtained for the ratio of the reduced probabilities of the proton and neutron transitions corresponds, to within the errors, to the single-particle value. At the same time, we observe a strong deviation of the probabilities of the proton transition in the nucleus $^{41}_{19}K_{22}$, whose core is not doubly magic, and of the neutron transition in $^{39}_{20}Ca_{19}$.

In the same table, we give the ratios of the reduced probabilities of proton $M2$ transitions of the type $1d_{3/2}$–$1f_{7/2}$ in the $_{21}$Sc isotopes to the probability of a neutron transition in $^{41}_{21}Ca_{21}$. At present, there are no data on the $M2$ transition in $^{41}_{21}Sc_{20}$, but it is obvious that for the Sc

TABLE VI. Ratios of reduced probabilities of transitions of a single proton or neutron (in accordance with Moszkowski's scheme).

L	1	2	3	4	5
$B(ML)^{M}_{p}/B(ML)^{M}_{n}$	1.44	1.66	1.77	1.84	1.88

isotopes from $A=49$ to $A=43$ the ratios of the reduced probabilities of the proton and neutron transitions increase. However, the ratio S^{p}_{W}/S^{n}_{W} for the nuclides $^{49}_{21}Sc_{28}$ and $^{41}_{20}Ca_{21}$ is very small despite the fact that these nuclei have a doubly magic core and one nucleon.

Reduced probabilities of $M4$ transitions

Sufficient experimental material has now been accumulated to permit comparison of proton and neutron transitions of the type $1h_{11/2}$–$2d_{3/2}$ of multipolarity $M4$. Neutron transitions of this type occur in isotones with $N=81$ in which Z varies from 52 to 66 (Ref. 18), and the proton transition occurs in the nucleus $^{207}_{18}Tl_{126}$ (Ref. 32). Experimental results are given in Table VIII and in Fig. 29. For transitions of the type $M4$, we observe a large deviation from the single-particle estimate of the given ratios of the reduced probabilities for nuclei with Z near 50 compared with nuclei near $Z=64$, for which the value is effectively equal to the estimate.

We shall only be able to gauge the importance of the influence of the doubly magic core on the reduced probabilities of $M4$ transitions in odd nuclei after the reduced probability $B(M4)$ of the transitions $1h_{11/2}$–$2d_{3/2}$ in ^{131}Sn has been determined.

Reduced probabilities of l-forbidden transitions in mirror nuclei

Besides the already considered case of $M2$ transitions in mirror nuclei, it is also interesting to compare the reduced probabilities of l-forbidden $M1$ transitions that oc-

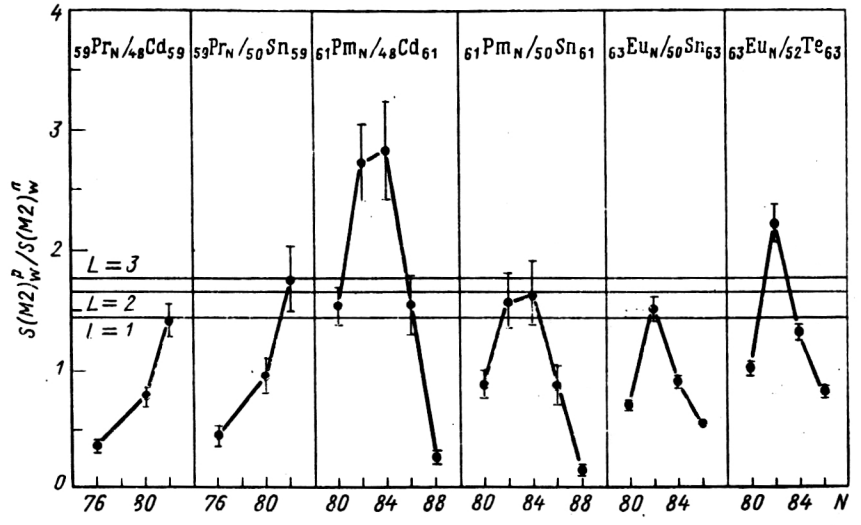

FIG. 28. Relative probabilities of proton and neutron transitions of the type $M2$ ($1h_{11/2}$–$1g_{7/2}$) in odd nuclei with a half-magic core near $N=Z=64$.

TABLE VII. Ratios of reduced probabilities for proton and neutron transitions of the type $M2$ $(1f_{7/2} \rightleftarrows 2d_{3/2})$.

Z^AN	E_i, keV	$2I_i^\pi$	S_W	S_W^p/S_W^n
$^{39}_{19}K_{20}$	2814	7−	3.1 (1)(−1)	1.29 (32)
$^{41}K_{22}$	1294	7−	9.8 (3)(−2)	0.41 (10)
$^{39}_{20}Ca_{19}$	2797	7−	2.4 (6)(−1)	—
$^{43}_{21}Sc_{22}$	152	3+	6.9 (1)(−2)	0.43 (5)
$^{45}Sc_{24}$	12	3+	4.7 (6)(−2)	0.29 (5)
$^{47}Sc_{26}$	767	3+	3.3 (1)(−2)	0.22 (3)
$^{49}Sc_{28}$	2371	3+	2.6 (−2)	0.18
$^{41}_{20}Ca_{21}$	2010	3+	1.6 (2)(−1)	—

cur in mirror nuclei having a common even–even core and ± 1 nucleon. It can be assumed in this case that if the structures of the excited states between which the l-forbidden transition takes place are identical, and the l-forbiddenness is lifted by the action of the same factors, then the ratio of the reduced probabilities of the proton and neutron transitions in the mirror nuclei must be close to the single-particle estimates. The known experimental data are given in Table IX (Refs. 24 and 33) and in Fig. 30. It should be noted that the ratios of the reduced probabilities of the l-forbidden $M1$ transitions in the mirror nuclei correspond, to within the errors, to the single-particle value, although the accuracy with which these ratios have been determined is not yet sufficiently good. The ratios $B(M1)_p/B(M1)_n$ are closest to the single-particle estimates for transitions that take place in mirror nuclei possessing an even–even core and $+1$ nucleon. This is obviously consistent with the assumption that in even–even nuclei with $N=Z$ shell closure occurs from $A=12$ to $A=40$. The largest deviations are observed for nuclei having an even–even core and -1 nucleon. This is the case for the pairs $^{31}_{15}P_{16}$–$^{31}_{16}S_{15}$ and $^{27}_{13}Al_{14}$–$^{27}_{14}Si_{13}$.

Reduced probabilities of l-forbidden $M1$ transitions in nonmirror nuclei for odd $N=Z$

In the previous subsection, we have considered the ratios of the reduced probabilities of l-forbidden $M1$ transitions in mirror nuclei. Table X (Ref. 34) gives data on other l-forbidden transitions of the same type in nonmirror nuclei. We note that in a number of cases these ratios differ appreciably from the single-particle estimates, a fact that may be due to the significant change in the structure of the considered states and the part played by the factors that influence the lifting of the l-forbiddenness. Only the ratio of the reduced probabilities of transitions for the nuclides $^{37}_{17}Cl_{20}$ and $^{33}_{16}S_{17}$ agree better with the single-particle estimates and with the ratio of the reduced probabilities of transitions in the mirror nuclei $^{33}_{17}Cl_{16}$–$^{33}_{16}S_{17}$ on closure of the neutron shell with $N=20$. As in the case of the $M2$ transitions, we observe an appreciable deviation from the single-particle estimates for the pair of nuclei $^{49}_{21}Sc_{28}$ and $^{41}_{20}Ca_{21}$. The appreciable increase of the ratio $B(M1)_p/B(M1)_n$ for the nuclei $^{45}_{21}Sc_{24}$–$^{41}_{20}Ca_{21}$ could be explained by the closure of the neutron subshell with $N=24$ that was manifested in the chain of $_{18}Ar$ and $_{22}Ti$ isotopes (see Fig. 15).

It is important to extend further the investigations of

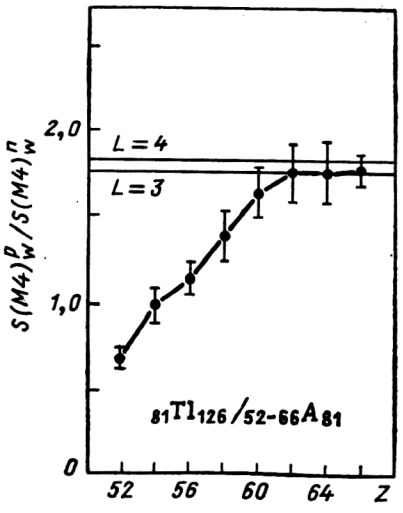

FIG. 29. Relative probabilities of proton and neutron transitions of the type $M4$ $(1h_{11/2}$–$2d_{3/2})$ in odd nuclei for $Z=N=81$.

TABLE VIII. Ratios of reduced probabilities of proton and neutron transitions of the type $M4$ $(1h_{11/2} \rightarrow 2d_{3/2})$.

Z^AN	E_i (E_f), keV	S_W	S_W^p/S_W^n
$^{207}_{81}Tl_{126}$	1348 (0)	3,2 (3)	—
$^{133}_{52}Te_{81}$	334 (0)	4,8 (1)	0,67 (6)
$^{135}_{54}Xe$	528 (0)	3,2 (1)	1,00 (10)
$^{137}_{56}Ba$	662 (0)	2,8 (1)	1,14 (11)
$^{139}_{58}Ce$	754 (0)	2,3 (1)	1,39 (14)
$^{141}_{60}Nd$	757 (0)	1,96 (3)	1,63 (16)
$^{143}_{62}Sm$	754 (0)	1,83 (6)	1,75 (17)
$^{145}_{64}Gd$	749 (27)	1,83 (6)	1,75 (17)
$^{147}_{66}Dy$	751 (72)	1,8 (1)	1,78 (10)

TABLE IX. Ratios of reduced probabilities of proton and neutron l-forbidden $M1$ transitions of the type $2s_{1/2} \leftrightarrows 1d_{3/2}$ in mirror nuclei.

ZA_N	E_i (E_f), keV	$2I_i^\pi$	S_W	$B(M1)_p/B(M1)_n$
$^{25}_{13}Al_{12}$ $^{25}_{12}Mg_{13}$	945 (451) 975 (585)	3^+ 3^+	2,4 (6) (−2) 1,5 (1) (−2)	1,60 (41)
$^{27}_{13}Al_{14}$ $^{27}_{14}Si_{13}$	1014 (844) 957 (780)	3^+ 3^+	8,7 (5) (−2) 1,9 (6) (−1)	0,44 (14)
$^{29}_{15}P_{14}$ $^{29}_{14}Si_{15}$	1383 (0) 1273 (0)	3^+ 3^+	5,8 (9) (−2) 3,7 (3) (−2)	1,57 (27)
$^{31}_{15}P_{16}$ $^{31}_{16}S_{15}$	1266 (0) 1249 (0)	3^+ 3^+	1,9 (1) (−2) 2,0 (5) (−2)	0,95 (24)
$^{33}_{17}Cl_{16}$ $^{33}_{16}S_{17}$	810 (0) 841 (0)	1^+ 1^+	3,4 (6) (−2) 2,9 (1) (−2)	1,17 (21)
$^{39}_{19}K_{20}$ $^{39}_{20}Ca_{19}$	2522 (0) 2469 (0)	1^+ 1^+	1,5 (6) (−2) 0,9 (1) (−2)	1,62 (65)

l-forbidden transitions in nonmirror nuclei with $N=Z$ in order to clarify the influence of closed shells on the probabilities of proton and neutron transitions. We give now examples of nuclei for which study of transitions of the same type is of particular interest. They are possible pairs of nuclides for study of the ratio of the reduced probabilities of transitions of the same type occurring in these nuclei:

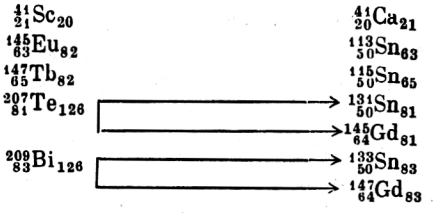

4. NEUTRON SHELL WITH $N=64$

Some experimental data relating to closure of a shell with $N=64$ were systematized in Ref. 14. We compare the properties of the nucleus $^{114}_{50}Sn_{64}$ with other doubly magic nuclides, paying particular attention to the comparison of its properties with the properties of the nucleus $^{146}_{64}GD_{82}$.

The arguments that justified the magic nature of the number $Z=64$ reduced basically to consideration of the following properties of the nuclei: the energies of the lowest states with spins 2_1^+ and 3_1^- in even–even nuclei with $N=82$; the energy gap in the proton system; the value of the proton pairing energy; the details of α decay (jump in the energies of the α particles on crossing of the shell at $Z=64$ and observation of a minimum in the reduced α width at $Z=64$), and also some other properties.

The results of theoretical calculations leading to the same conclusion demonstrated the vanishing of the function of the superfluid pairing correlations for ^{146}Gd and explained several properties of even–even and odd nuclei by assuming a magic nature of the nucleus ^{146}Gd (Ref. 5). The properties of the tin isotopes are especially interesting, since they have a closed proton shell with $Z=50$ and neutron number that varies from $N=50$ to $N=82$. This circumstance makes it possible to hope for detection of effects associated with closure of neutron shells and subshells.

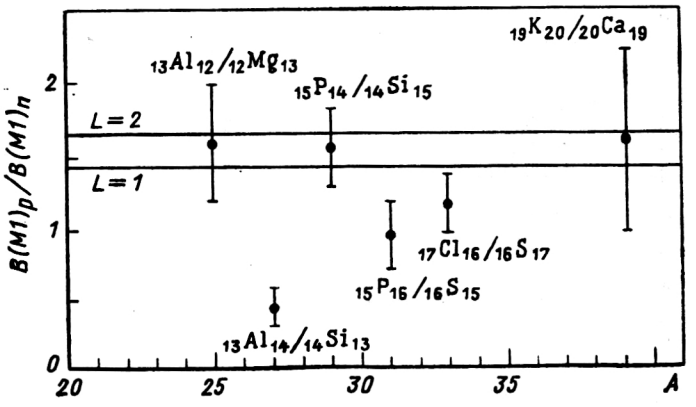

FIG. 30. Relative probabilities of l-forbidden proton and neutron transitions of type $M1$ in mirror nuclei.

TABLE X. Ratios of reduced probabilities of proton and neutron l-forbidden $M1$ transitions in nonmirror nuclei.

Z^AN	$E_i(E_f)$, keV	$2I_i^\pi$	$B(M1)$, μ_N^2	$B(M1)_p/B(M1)_n^*$
		$2s_{1/2} \rightleftarrows 1d_{3/2}$		
$^{31}_{15}P_{16}$	1266 (0)	3^+	3,44 (20) (−2)	0,52 (8) (0)
$^{33}_{15}P_{18}$	1431 (0)	3^+	2,29 (31) (−2)	0,35 (7) (−2)
$^{29}_{14}Si_{15}$	1273 (0)	3^+	6,62 (95) (−2)	—
$^{35}_{17}Cl_{18}$	1219 (0)	1^+	1,43 (19) (−1)	2,57 (35) (0)
$^{37}_{17}Cl_{20}$	1726 (0)	1^+	5,63 (92) (−2)	1,01 (17) (0)
$^{33}_{16}S_{17}$	841 (0)	1^+	5,56 (14) (−2)	—
$^{43}_{21}Sc_{22}$	855 (152)	1^+	4,1 (6) (−4)	2,01 (52) (−2)
$^{45}_{21}Sc_{24}$	939 (12)	1^+	0,65 $(^{+51}_{-28})$ (−2)	0,32$^{+25}_{-14}$ (0)
$^{47}Sc_{26}$	1391 (767)	1^+	0, 58 (−2)	0,29 (0)
$^{49}Sc_{28}$	2371 (2228)	3^+	6,7 (4) (−4)	3,30 (8_0) (−2) **
$^{41}_{20}Ca_{21}$	2670 (2010)	1^+	2,03 (48) (−2)	—
		$3s_{1/2} \rightleftarrows 2d_{3/2}$		
$^{207}_{81}Tl_{126}$	351 (0)	3^+	2,29 (53) (−2)	—
$^{139}_{58}Ce_{81}$	255 (0)	1^+	1,59 (30) (−2)	1,44 (43) (0) **
$^{145}_{64}Gd_{81}$	27 (0)	3^+	0,79 (2) (−2)	2,90 (67) (0)

*In the calculation of the error in $B(M1)_p/B(M1)_n$ we took into account only the error in the determination of the lifetime of the corresponding state.

**In the calculation of these ratios the statistical factor was not taken into account.

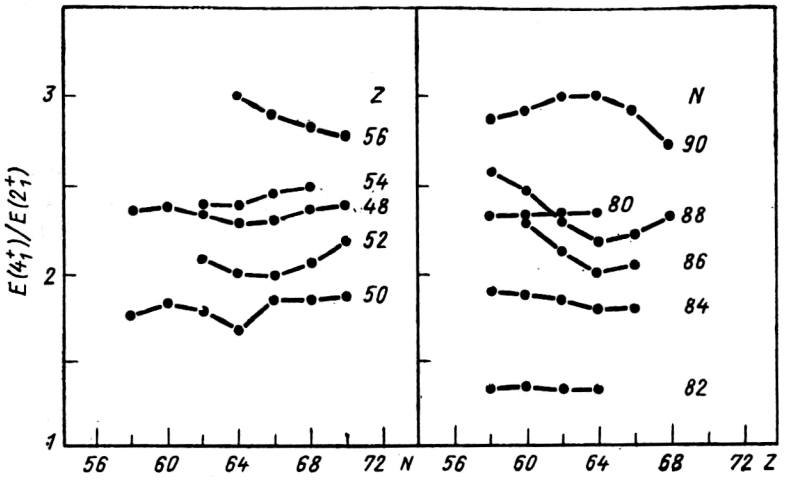

FIG. 31. Dependence of $E(4_1^+)/E(2_1^+)$ on N for nuclei near $Z=N=64$.

TABLE XI. Systematics of the ratios $E(4_1^+)/E(2_1^+)$ in doubly magic nuclei and in the nucleus ^{114}Sn.

Nucleus	$^{16}_{8}O_8$	$^{40}_{20}Ca_{20}$	$^{48}_{20}Ca_{28}$	$^{56}_{28}Ni_{28}$	$^{90}_{40}Zr_{50}$	$^{114}_{50}Sn_{64}$	$^{132}_{50}Sn_{82}$	$^{146}_{64}Gd_{82}$	$^{209}_{82}Pb_{126}$
$E(4_1^+)$, keV	10350	5280	4503	3924	3080	2188	4416	2612	4324 *
$E(2_1^+)$, keV	6917	3904	3832	2701	2186	1300	4041	1971	4085
$E(4_1^+)/E(2_1^+)$	1,50	1,35	1,17	1,45	1,41	1,69	1,09	1,32	1,06

*K. Sistemich, Report IFJN 1302/PS, Krakow, 1985, p. 142.

TABLE XII. Values of proton and neutron gaps above different closed shells.*

Nucleus	$^{40}_{20}Ca_{20}$	$^{90}_{40}Zr_{50}$	$^{114}_{50}Sn_{64}$	$^{132}_{50}Sn_{82}$	$^{146}_{64}Gd_{82}$	$^{208}_{82}Pb_{126}$
$\Delta(p)$, keV	7244 (3)	3198 (6)	4744 (20)	5676 (300)	3440 (58)	4206 (7)
$\Delta(n)$, keV	7280 (5)	4777 (7)	2754 (17)	5860 (280)	3870 (20)	3432 (4)

*The data for all nuclei except ^{114}Sn are taken from Ref. 4.

Energies of excited states of magic even–even nuclei

For the Sn isotopes, the energy of the 2_1^+ state is observed to rise as the number N is increased to 64, and there is a simultaneous lowering of the energy of the 3_1^- state. Such behavior is characteristic of shell closure in other magic nuclei.

Let us consider the behavior of the first excited 2_1^+ and 3_1^- states (Fig. 8). In ^{114}Sn, the $I^\pi = 2_1^+$ level is lowest, just as is the position of the analogous levels in the doubly magic nuclei ^{90}Zr and ^{132}Sn, whereas in ^{146}Gd and ^{208}Pb the $I^\pi = 3_1^-$ level is the lowest.

Consequences of closure of neutron shells can also be seen by examining the dependence of $E(4_1^+)/E(2_1^+)$ on N (Fig. 31). This ratio reaches a minimum at $N = 64$, this being similar to the behavior of the analogous ratio on closure of the neutron shells with N equal to 82 and 126 for doubly magic nuclei (Table XI). Evidence for enhanced stability of this neutron shell is the presence of a minimum at $N = 64$ for nuclei with Z equal to 48, 52, 54 as well. An analogy is also observed in the change in the shape of the nuclei when the shells with $N = 64$ and $Z = 64$ are crossed. In both cases the shape of the nucleus changes from spherical to ellipsoidal on corresponding changes in the number of neutrons or protons. A difference between ^{114}Sn and other doubly magic nuclei is the lower energy of the 2_1^+ and 3_1^- states, corresponding to the greater collectivization of these states.

The energy gap in ^{114}Sn

Table XII gives experimental data on energy gaps—proton and neutron—in doubly magic nuclei and in ^{114}Sn. The gap is defined as the difference between the separation energies for a neutron or proton:

$$\Delta(n) = S_n(^{115}\text{Sn}) - S_n(^{114}\text{Sn});$$

$$\Delta(p) = S_p(^{115}\text{Sb}) - S_p(^{114}\text{Sn}).$$

Data on the separation energies of the corresponding nucleons or pairs of nucleons were taken from Ref. 11. The value of Δn for ^{114}Sn is the smallest for the considered set of nuclei, although it differs from the value for ^{208}Pb by only 20%. However, the small neutron gap in ^{114}Sn does not lead to complete destruction of the shell at $N = 64$, this being evidently due to the stabilizing influence of the closed proton shell with $Z = 50$.

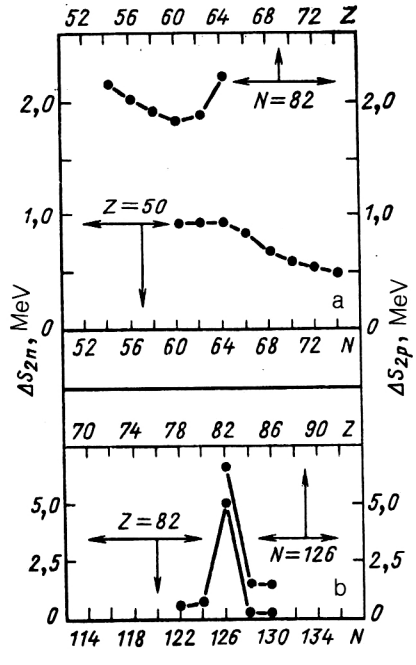

FIG. 32. Two-nucleon binding energies: a) for nuclei in the region of $Z=N=64$; b) for nuclei in the region of $Z = 82$ (for $N = 126$) and $N = 126$ (for $Z = 82$).

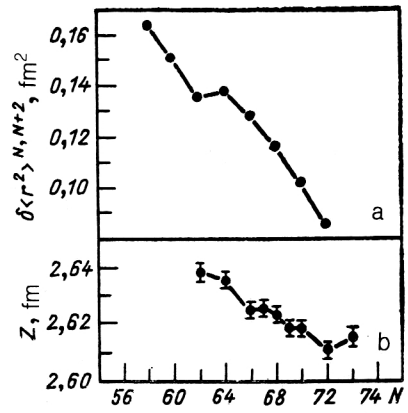

FIG. 33. Change of the mean-square radii of Sn isotopes (a) (Ref. 14) and reduced width of the nuclear surface layer of Sn isotopes (b).[15]

Binding energies of two neutrons

The binding energies of two neutrons also characterize the effect of the closure of neutron shells. The effect is most clearly manifested when one analyzes $\Delta S_{2n}=S_{2n}(Z,N)-S_{2n}(Z,N+2)$. Figure 32a shows the dependence of the difference of the two-neutron binding energy on the number of neutrons for the Sn isotopes. For comparison, we also give the analogous dependence of the two-proton binding energy for the nuclei adjacent to ^{146}Gd. It is obvious that the number $N=64$ is distinguished in the nuclei with $Z=50$. The nature of the dependence of ΔS_{2n} and ΔS_{2p} near $N=64$ and $Z=64$ is similar, though it is very different from the same dependence at the closure of the shells with the strong magic numbers $Z=82$ and $N=126$ (Fig. 32b).

Energies of α decay and other nuclear properties

It was shown in Ref. 11 that in the α decays ${}^{115}_{50}\mathrm{Sn}_{65}(\alpha){}^{111}_{48}\mathrm{Cd}_{63}$ and ${}^{119}_{52}\mathrm{Te}_{67}(\alpha){}^{115}_{50}\mathrm{Sn}_{65}$ enhanced stability of ^{115}Sn is observed. The α-decay energy was found to be about 200 keV greater than expected from interpolation of the decay energy between the neighboring nuclei. This effect near $N=64$ is similar to the effect on closure of the $Z=64$ shell, though it is expressed less clearly. Usually, the difference in the α-decay energies between even–even isotones in the region adjoining $Z=64$ is $\sim$0.5 MeV, and the difference between the isotones Dy($Z=66$) and Gd($Z=64$) is approximately 1.1 MeV (Ref. 35).

There is other evidence for closure of the neutron subshells $1g_{7/2}$ and $2d_{5/2}$. For example, there is the abrupt change of the mean-square radii at $N=64$ (Refs. 30–38): $\delta\langle r^2\rangle^{N,N+2}=\langle r^2\rangle(A)-\langle r^2\rangle(A+2)$ (Fig. 33a) both for the isotopes of the element with $Z=50$ and for the isotopes of the elements with $Z=48$, 49. The same circumstance can evidently also explain the pronounced decrease of the reduced thickness of the nuclear surface layer on the transition from $N=64$ to $N=66$ in the even–even Sn isotopes (Fig. 33b).[15]

In addition, closure of the subshell with $N=64$ was also found[39] to influence the magnetic moments of some odd iodine isotopes.

On the magic nature of the number $N=64$

The available experimental data obviously indicates closure of a neutron subshell with $N=64$ when the orbitals $1g_{7/2}$ and $2d_{5/2}$ are occupied. The properties of nuclei with $N=64$ are very largely the same as those of the nuclei with a proton subshell $Z=64$. The similarity can be traced in the systematics of the energies of the excited states of even–even nuclei, in the energy gaps, in the two-particle (proton or neutron) binding energies, in the α-decay energies, in the properties of the neighboring odd nuclei, and in the probabilities of electromagnetic transitions. It should be noted that closure of subshells of nucleons of a definite type is most clearly manifested when a magic shell of nucleons of the opposite type is closed.

A feature of the magic nature of the nuclei with $N=64$, as in the case $Z=64$, is that it has a more local nature, even compared with the $Z=64$ subshell. This was confirmed in Ref. 39, in which it was shown that the influence of closure of the subshell with $N=64$ on the magnetic moments of the iodine ground states disappears already on the addition of four valence protons.

Another characteristic feature of the closure of the neutron subshell with $N=64$ is the high collectivization of the 2_1^+ and 3_1^- states of ^{114}Sn compared with the other tin isotopes. This is reflected in an increase in the probability of electric monopole, quadrupole, and octupole transitions. This last circumstance is determined by the presence of appreciable deformation, $\beta_2=0.17$, in the region of $N=64$. The apparent contradiction between the values found for the deformation parameter β_2 by the isotopic-shift method and from Coulomb excitation was analyzed in Ref. 37. The contradiction can be eliminated by assuming that the considered tin isotopes have an octupole deformation; this is consistent with experimental results on the reduced probabilities $B(E3)$ of transitions from octupole states (see Table IV).

Occupation of orbitals by pairs of neutrons in tin isotopes is rather clearly expressed and to a considerable degree resembles the closure of neutron shells in deformed nuclei, which is most probably associated with the coexistence of shapes in a nucleus. However, the number $N=64$ is to a certain extent distinguished from other neutron numbers in this region, since it is the one that most fully fits the single-particle scheme of the shell model. Besides the facts already considered, we can mention as the most characteristic features of this phenomenon the closeness to the single-particle limit of the relative transition probabilities $B(M2)_n/B(M2)_p$ in ${}^{145}_{63}\mathrm{Eu}_{82}$ and ${}^{113}_{50}\mathrm{Sn}_{63}$ and the demonstration of closure of the shell with $N=64$ by hole states in the odd tin isotopes. The identity of a number of properties of nuclei with $N=64$ and $Z=64$ is evidence for a magic nature of the number with $N=64$, though theoretical calculations must be made before a definitive conclusion is drawn.

CONCLUSIONS

Differentiation of the energy surface of excited states of nuclei of a definite nature and given spin has been shown to be the method that permits detection of closure of neutron and proton shells and subshells in spherical even–even and odd nuclei, and also the closure of quasishells in the deformed and transitional regions of nuclei. The most important consequence of our analysis is the discovery that states of a definite nature and definite spin are selectively sensitive to shell closure in nuclei, i.e., the discovery that closed shells affect the energy of certain states but not the energy of others. Therefore, the question of the influence of shell closure on certain properties of excited nuclear states cannot be settled without detailed study of the structure of these states. This is indicated by the results of Ref. 13, in which α decay of Pb isotopes was studied, and it was shown that the proton number $Z=82$ is not magic for nuclei in the region $N=104$–110 (Fig. 10). This conclu-

sion follows from analysis of the values of the reduced widths of α transitions.

Another interesting fact is the establishment of closure of shells in light even–even nuclei when $N=Z$.

The discovery in deformed nuclei of successive occupation of shells by nucleon pairs will evidently reveal lifting of level degeneracy in the transitional region of nuclei and will effectively solve the problem of coexistence of shapes in a nucleus.

It is necessary to point out that magnetic transitions of the type $M1$, $M2$, $M4$ can serve as a probe permitting detection of shell and subshell closure in nuclei. An important circumstance characterizing the limits of applicability of the single-particle model in explaining the relative probabilities of proton and neutron magnetic transitions of the same type is the demonstration that the ratios of the probabilities of proton and neutron transitions for nuclei possessing an even–even magic core and ± 1 nucleon correspond to the single-particle limit. This means that an electromagnetic transition in an odd nucleus with a doubly magic core is equivalent in a certain approximation to an electromagnetic transition of a single nucleon.

It would be very interesting to extend the systematics of the relative probabilities of proton and neutron transitions of the same type in odd nuclei possessing a doubly magic core and ± 1, ± 3 nucleons. This could help to determine the range of influence of the magic numbers and predict the probabilities of related proton and neutron transitions in different nearly magic nuclei. Analysis of the relative probabilities of magnetic transitions in nearly magic nuclei has a direct bearing on the problem of nuclear magnetism and the polarization of nuclear matter.

I thank S. Briancon and É. Khudaĭberdyev for collaboration at certain stages of this work and K. Ya. Gromov for a number of critical comments.

[1] M. Goeppert Mayer and J. H. D. Jensen, *Elementary Theory of Nuclear Shell Structure* (Wiley, New York, 1955).
[2] W. D. Schmidt-Ott and K. S. Toth, Phys. Rev. C **13**, 2574 (1976).
[3] P. Kleinheinz, R. Broda, P. J. Daly *et al.*, Z. Phys. A **290**, 279 (1979).
[4] G. D. Alkhazov, N. Ganbaatar, K. Ya. Gromov *et al.*, Preprint No. 1135 [in Russian], Leningrad Institute of Nuclear Physics, Leningrad (1985).
[5] S. A. Artamonov, V. I. Isakov, S. G. Ogloblin *et al.*, Yad. Fiz. **39**, 328 (1984) [Sov. J. Nucl. Phys. **39**, 206 (1984)].
[6] S. A. Artamonov, V. I. Isakov, S. G. Ogloblin *et al.*, in *Nuclear Physics. Proc. of the 20th Winter School of the Leningrad Institute of Nuclear Physics* [in Russian] (Leningrad, 1985), p. 11.
[7] M. S. Antony, Nuovo Cimento **91A**, 217 (1976).
[8] V. G. Soloviev, *Theory of Complex Nuclei* (Pergamon Press, Oxford, 1976) [Russ. original, Nauka, Moscow, 1971].
[9] A. Bohr and B. R. Mottelson, *Nuclear Structure*, Vol. 1 (Benjamin, New York, 1969) [Russ. transl., Mir, Moscow, 1971].
[10] J. Mattauch, W. Thiele, and A. Wapstra, Nucl. Phys. **67**, 1 (1965).
[11] A. Wapstra and G. Audi, Nucl. Phys. **A432**, 55 (1985).
[12] M. Goeppert Mayer and J. H. D. Jensen, in *Alpha-, Beta-, and Gamma-Ray Spectroscopy*, edited by K. Siegbahn (North-Holland, Amsterdam, 1965) [Russ. transl., Atomizdat, Moscow, 1969].
[13] K. S. Toth, Y. A. Ellis-Akovali, C. R. Binghan *et al.*, Phys. Rev. Lett. **53**, 1623 (1984).
[14] M. S. Antony and J. Britz, Preprint CRN/PN 86-0 (1986).
[15] J. R. Ficenec, L. A. Fajardo, W. P. Trower *et al.*, Phys. Lett. **42B**, 213 (1972).
[16] E. Erba, U. Facchini, and H. Saetta-Menichella, Nuovo Cimento **22**, 1237 (1961).
[17] M. Sakai, At. Data Nucl. Data Tables **31**, 399 (1984).
[18] K. S. Toth, Y. A. Ellis-Akovali, F. T. Avignone *et al.*, Phys. Rev. C **32**, 342 (1985).
[19] J. Bonn, G. Huber, H. J. Kluge *et al.*, Z. Phys. A **276**, 203 (1976).
[20] A. Bäcklin, N. G. Jonsson, R. Julin *et al.*, Nucl. Phys. **A351**, 490 (1981).
[21] L. K. Peker, Nucl. Data Sheets **43**, 579 (1984).
[22] L. K. Peker, Nucl. Data Sheets **41**, 195 (1984).
[23] M. J. Martin, Nucl. Data Sheets **47**, 797 (1986).
[24] P. M. Endt, At. Data Nucl. Data Tables **26**, 47 (1981).
[25] B. Harmatz, Nucl. Data Sheets **30**, 413 (1980).
[26] J. K. Tuli, Nucl. Data Sheets **29**, 533 (1980).
[27] M. E. Voĭkhanskiĭ, in *Gamma Rays* [in Russian] (USSR Academy of Sciences, Moscow–Leningrad, 1951), p. 5.
[28] P. M. Endt and C. Van Der Leun, Nucl. Phys. **A310**, 1 (1978).
[29] P. M. Endt, At. Data Nucl. Data Tables **23**, 3 (1979).
[30] P. M. Endt, At. Data Nucl. Data Tables **23**, 547 (1979).
[31] T. W. Burrows, Nucl. Data Sheets **48**, 569 (1986).
[32] M. R. Schmorak, Nucl. Data Sheets **43**, 383 (1984).
[33] T. K. Alexander and G. C. Ball, Preprint AECL-9262 (1986).
[34] N. A. Bonch-Osmolovskaya, V. A. Morozov, M. A. Dolgopolov, and M. A. Kopytin, Fiz. Elem. Chastits At. Yadra **18**, 739 (1987) [Sov. J. Part. Nucl. **18**, 313 (1987)].
[35] K. S. Toth, in *Proc. of the Fourth Intern. Conf. on Nuclei Far from Stability*, Vol. II (CERN 81-09, 1981), p. 551.
[36] R. Wenz, A. Timmermann, and E. Mathias, Z. Phys. A **303**, 87 (1981).
[37] J. Eberz, U. Dinger, G. Huber *et al.*, Z. Phys. A **326**, 121 (1987).
[38] H. Lochmann, J. Eberz, G. Huber *et al.*, Sci. Rep. GSI-85-1 (1985), p. 79.
[39] V. B. Green, N. J. Stone, T. L. Shaw *et al.*, Phys. Lett. **173B**, 115 (1986).
[40] V. A. Morozov, Brief Communication No. 7 33-88, JINR, Dubna (1988).
[41] V. A. Morozov, Brief Communication No. 7 33-88, JINR, Dubna (1988).

Translated by Julian B. Barbour